EUROPEAN ORGANIZATION FOR NUCLEAR RESEARCH

HADRONIC FINAL STATES IN MUON-INDUCED REACTIONS*)

C.A. Heusch**)

CERN, Geneva, Switzerland
and
Sektion Physik, Universität München, Munich, Germany

Geneva - 9 July 1975

Invited talk at the
EPS International Conference on High-Energy Physics,
Palermo, Italy, 23-28 June 1975

---

*) Work supported in part by the U.S. Energy Research and Development Administration.

**) Permanent address: University of California, Santa Cruz, California, USA.

HADRONIC FINAL STATES IN MUON-INDUCED REACTIONS*)

C.A. Heusch**)

CERN, Geneva, Switzerland
and
Sektion Physik, Universität München, Munich, Germany

1. REMEMBER SCALING?

In 1968, Bjorkén had speculated that, as energies of available lepton beams increased, a regularity of scattering cross-sections was to emerge, manifesting itself as an energy independence of the inelastic nucleon form factors W_1 and (ν times) W_2.

Very soon after, experiments performed at the SLAC spectrometer facility showed that, remarkably, this scaling behaviour expected for asymptotically high momentum transfers and energies showed up at astonishingly low kinematical parameters: for $Q^2 \gtrsim 0.5$ (GeV/c)^2, $\nu = E - E' \gtrsim 2$ GeV, the measured structure functions appear to be functions only of ν/Q^2, irrespective of energy.

The photon, mediator of these lepton-hadron collisions, thus effects hadronic final states adding up to an astonishing energy independence, while at the same time changing its negative (mass)^2 through a very large range. In fact, the "hadronic component" of the virtual photon, while decidedly different from that of the $Q^2 = 0$ real photon, may not change much once the total hadronic mass is above the "nucleon resonance region" ($W \gtrsim 2.2$ GeV), its own mass $Q^2 \equiv -q^2 > 0.5$ (GeV/c)^2. How can we trace its behaviour in terms of individual reaction components?

In a vector dominance picture, the photon's hadronic part is a linear combination of ρ^0, ω^0, ϕ^0 states, with couplings prescribed by unitary symmetry schemes. In this framework,

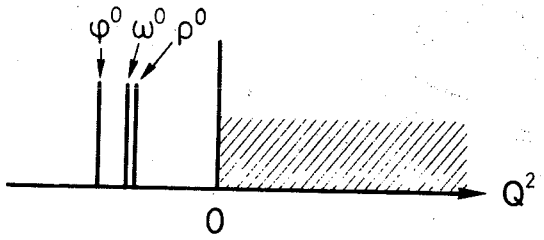

going from the photoproduction ($Q^2 = 0$) to the electroproduction ($Q^2 > 0$) picture just means moving somewhat further away from the poles at m^2 (ρ^0, ω^0, ϕ^0) at $Q^2 < 0$, already quite remote. As Q^2 increases, changes observed between $Q^2 = 0$ and small positive Q^2 values would be expected to increase in size.

In fact, results of lepton production experiments presented at the Bonn (1973) and London (1974) Conferences hinted that only two measured quantities, each particularly telling for one deeply-inelastic-scattering model, displayed continuing Q^2 dependence,

---

*) Work supported in part by the U.S. Energy Research and Development Administration.

**) Permanent address: University of California, Santa Cruz, California, USA.

whereas such characteristic inclusive features as the charged hadron multiplicity $\langle n \rangle$, the fractional topological cross-sections for the production of n charged hadrons σ_n/σ_{tot}, and the average transverse momentum of final-state hadrons $\langle p_\perp \rangle$, exhibit little if any Q^2 dependence between $Q^2 = 0.3$ and the highest values studied. These Q^2-dependent quantities are the slope parameter b of the diffractive peak of elastic vector meson production:

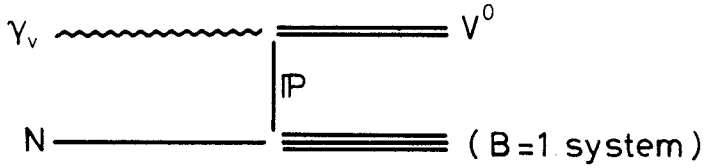

$$\frac{d\sigma}{dt}(\gamma_v p \to V^0 p) \sim e^{bt}$$

where a flattening of the peak with Q^2 has been touted as the "shrinking photon" indicator; and the ratio of positively to negatively charged forward-emitted hadrons $R = \pi^+/\pi^-$. In the conventional quark-parton picture,

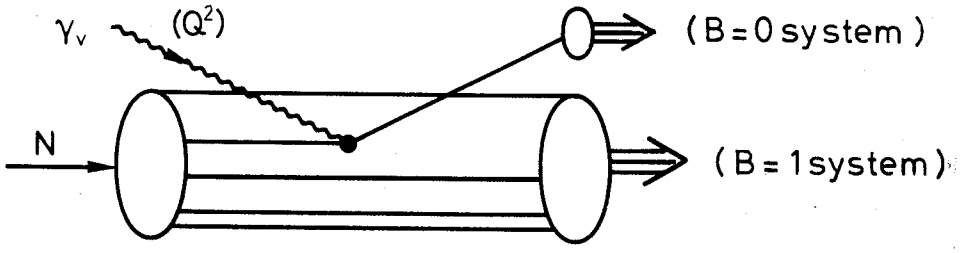

where the photon couples to the charge of the parton, the leading p quark would be expected to strongly favour the emergence of positive hadrons.

Today, it appears that this picture needs some correcting: the photon shrinking is a possibility at best, and the forward charge ratio may reach a plateau much earlier than we expected a year ago.

To reach fuller results on the details of hadronic final states in deeply inelastic lepton scattering, the following points have to be watched:

- detect the full final state: $\sim 4\pi$ acceptance;
- minimize radiative effects: μ beams will be preferable to e beams;
- optimize beam properties to define initial state precisely;
- produce a statistically meaningful sample: large luminosity, low trigger rate.

2. EXPERIMENT

The U.C. Santa Cruz/SLAC Group D Collaboration[1], on whose data I am basing this report, therefore first concentrated on the construction, at the Stanford Linear Accelerator Center, of a high-quality muon beam. Its properties are the following[2]:

μ^+: energy 14 GeV
resolution: $\Delta p/p = 1\%$, $\Delta\Theta = 2$ mrad
spot size at target: $\sigma_x = \sigma_y = 5$ mm
intensity $\lesssim 10^5$ μ/sec (actually used $\sim$ 200/1.5 μsec SLAC pulse)
halo: $\sim$ 1% over streamer chamber cross-section
hadron admixture: $\pi/\mu = (4 \pm 1.5) \times 10^{-5}$.

The "cost" of producing one muon into our beam phase space is high: since (Fig. 1) it takes a sequence of high-energy bremsstrahlung and highly asymmetric μ pair production to start a muon on its way through a series of filters, collimators, and a three-focus beam line, one muon at our target corresponds to some 10^9 fully (20 GeV) accelerated electrons.

The experiment set-up is schematically shown in Fig. 2: The muon beam is incident on a 40 cm long, 2 cm diameter liquid hydrogen target inside a 2 m long streamer chamber, which is immersed in a 16 kG magnetic field. The streamer chamber[3] was desensitized in a small region around the target; it contains absorbing fins for δ-ray interception above and below the target; the non-interacting beam traversed the chamber body inside a 5 cm diameter helium-filled plastic tube. These features, while introducing only small inefficiencies into the final-state detection, permitted a muon flux of up to 400 muons per memory time of the chamber to be employed. A trigger for this chamber and for a three-camera system is provided simply by a muon scattered appreciably out of the beam phase space and traversing a 1.5 m lead filter in addition to appropriate hodoscope combinations. The trigger was optimized for Q^2 values 0.5 to 5, energy losses $2 \leq \nu \leq 12$, and reached a geometric efficiency between 60 and 90%. The trigger cross-section was about 10 μb, some 15 times the event rate. We assembled a data sample of some 15,000 events in H_2 (of which ∿ 8,000 deeply inelastic), 25,000 (∿ 14,000) in D_2. The data analysis is nearly complete on the H_2 sample.

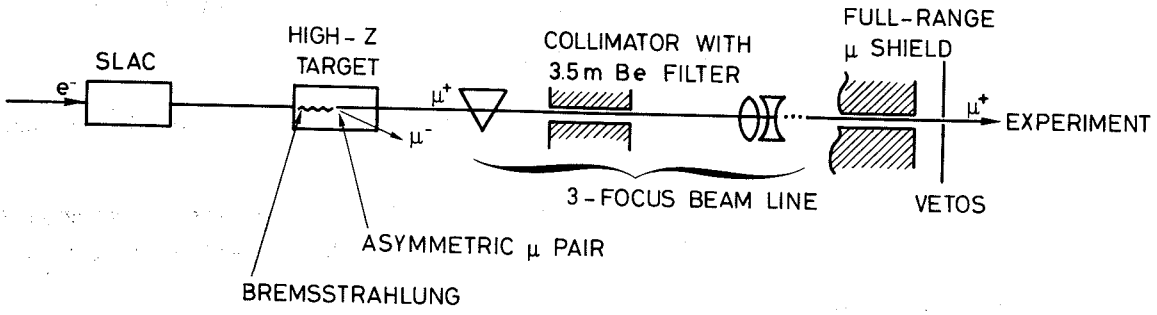

Fig. 1

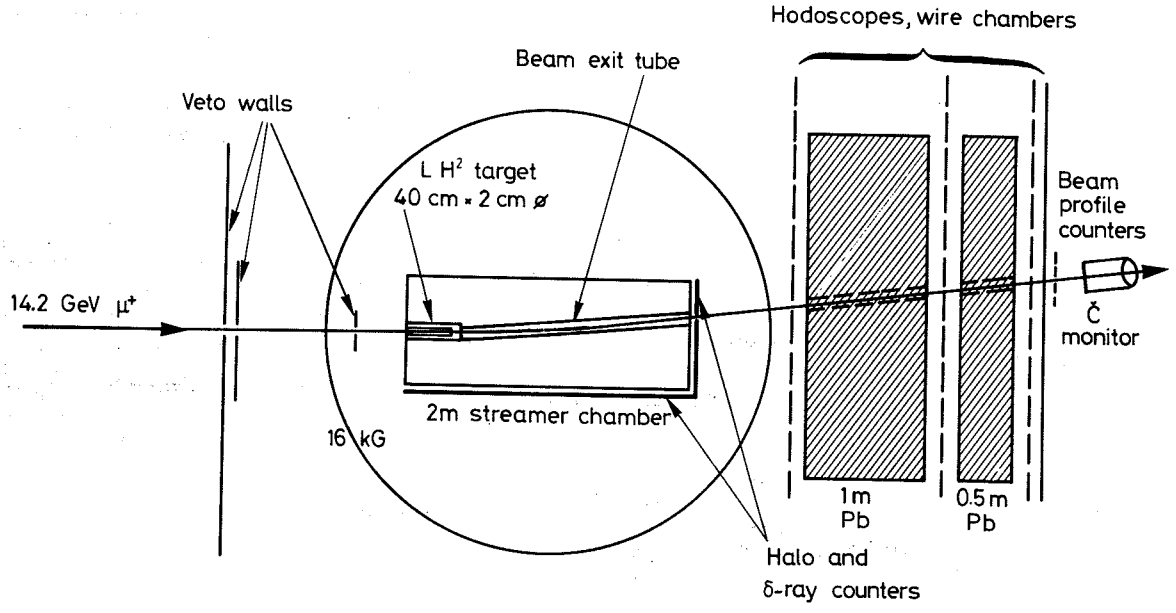

TOP VIEW OF E - 72 LAYOUT SCHEME

Fig. 2

3. RESULTS

I will today concentrate on our results concerning those features I mentioned above, starting with fractional topological cross-sections, for which we now present final data (Fig. 3). Through three different $W = \sqrt{s}$ bins, you can clearly distinguish these features (remembering that, by charge conservation, $n = 1, 3, 5, \ldots$, for the process $\gamma_V p \to$ hadrons)

- the events containing one charged hadron in the final state make up a much larger fraction of σ_{tot} in electroproduction than in photoproduction (dashed line);
- the opposite is true for 3-prong events;
- there is no difference for $Q^2 = 0$, $Q^2 > 0$ in the 5,7-prong sample;
- the change occurs rapidly between $Q^2 = 0$ and $Q^2 \simeq 0.2$; there is no noticeable Q^2 dependence above 0.2.

How can this remarkable picture be understood in terms of the contributing processes? For the "one-prongs", these processes are principally

$$\left.\begin{array}{l}\gamma_V p \to \pi^0 p \\ \qquad\ \pi^+ n \\ \qquad\ \Delta^+ \pi^0 \\ \qquad\ \Delta^0 \pi^+ \quad (\Delta^0 \to n\pi^0)\end{array}\right\} + \text{neutrals}\ .$$

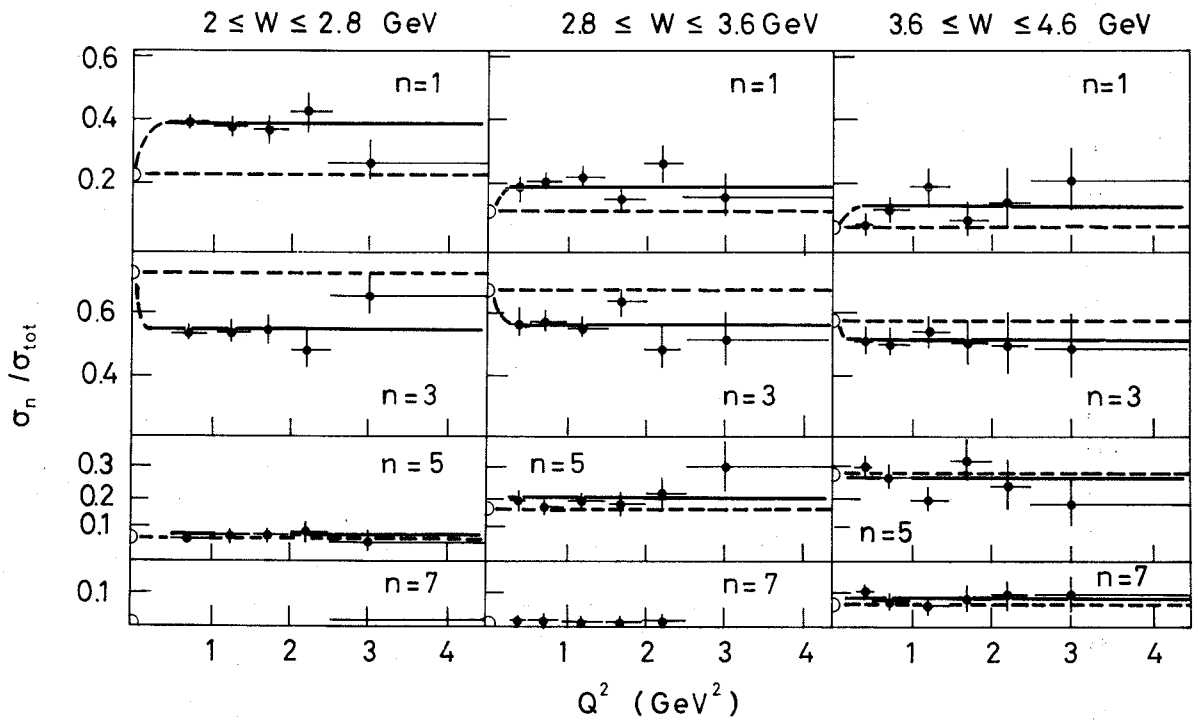

Fig. 3

The only phenomenon we know to occur in the small Q^2 range, where σ_1/σ_{tot} jumps from 0.2 to 0.4 in the lowest W bin, is the turn-on of the longitudinal photon component. The $n\pi^+$ channel, dominated by π exchange, is known to profit from this; the $p\pi^0$ channel most probably not[4]. Can the $n\pi^+$ channel, which decreases rapidly with increasing Q^2, account for this drastic effect? Let us look at the "3-prongs", which show a sudden decrease by almost 20% between $Q^2 = 0$ and $Q^2 = 0.2$. They are made up of channels such as

$$\left.\begin{array}{l}\gamma_V p \to \pi^- \Delta^{++} \\ \quad\ \pi^+ \Delta^0 \ (\Delta^0 \to p\pi^-) \\ \quad\ p\rho^0 \\ \quad\ p\omega^0 \\ \quad\ p\phi^0\end{array}\right\} + \text{neutrals}\ .$$

Of these, the first channel also should profit from the turn-on of σ_ℓ. However, we found Δ^{++} production to be prominent only at the lowest W values. The vector meson channels are clearly the focus of our interest here. Do they explain the sudden drop-off, then constancy, of σ_3/σ_{tot}? At the 1973 Bonn Conference, Talman[5] had shown $\sigma_{\rho^0}/\sigma_{tot}$ results from different groups that varied widely, but appeared to indicate a continuing decrease with increasing Q^2.

From our final data sample, we took only the fully defined $p\pi^+\pi^-$ events to make simultaneous fits to the $\pi^-\Delta^{++}$, $\pi^+\Delta^0$, and $p\rho^0$ hypotheses, plus some phase-space contribution. A fairly background-free ρ sample emerges in all Q^2 bins (Fig. 4). From these data, we compute σ_ρ/σ_{tot}, and find it to be almost constant with Q^2 over the entire range covered here ($0.2 \leq Q^2 \leq 3$), only a gentle decrease being indicated. Figure 5 shows the change from the photoproduction value of $\sim$ 16% to the $Q^2 > 0.2$ value of $\sim$ 4 to 5%. It is not clear that this is compatible with the much-quoted Q^2 dependence of the ρ propagator $\sim (1 - Q^2/m_\rho^2)^{-2}$. Since longitudinal ρ^0 production is reported[6] to strongly increase with Q^2, the observed behaviour of σ_ρ/σ_{tot} requires some delicate balancing of longitudinal and transverse components.

From the same data, we determine the exponential slope parameter $b(Q^2)$ of the diffraction peak by fitting it to the form e^{bt} in the t range below 0.7 [since the peak flattens off with increasing t, comparisons of $b(Q^2)$ data from different experiments must take care to specify the t region of the fit]. Figure 6 gives our results for b in three Q^2 bins of roughly equal statistical significance, together with the inconclusive picture shown by Talman[5] two years ago. You see that the new data, extending much further out in Q^2 than the previously covered range, indicate an essentially flat behaviour of b at Q^2 values up to $\sim 3\ (\text{GeV/c})^2$. Since there is no agreement on the $b(Q^2 = 0)$ value that we might compare our values to, two possibilities remain open: either there is a sudden decrease of b from $\sim 8\ (\text{GeV/c})^{-2}$ at $Q^2 = 0$ to ~ 6 at $Q^2 \geq 0.2$, or there is essentially no change in b when we turn from photo- to electroproduction of ρ^0; in either case, any "shrinking of the photon" with increasing Q^2 cannot be established from these data, but will have to wait for experimental information spanning a much larger Q^2 range.

Before we discuss the implication of these findings on $\sigma_3/\sigma_{tot}\ (Q^2)$, let us look at "elastic" ω^0 production. From 1C fit samples with three charged hadrons, the invariant-mass distribution for the $\pi^+\pi^-\pi^0$ hypothesis contains clear and narrow ω^0 signals, shown in a representative way by Fig. 7. While the background subtraction becomes less model-dependent than in the ρ^0 case due to the narrow width of the ω^0, the less-constrained ω^0

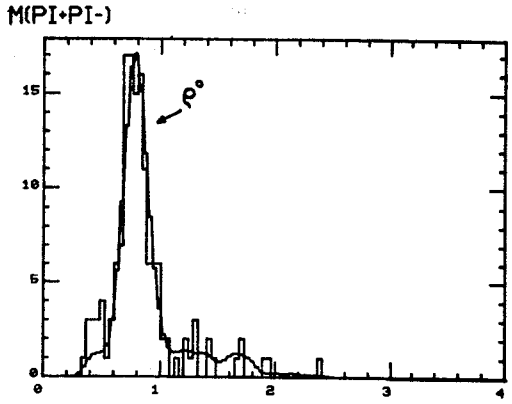

Fig. 4

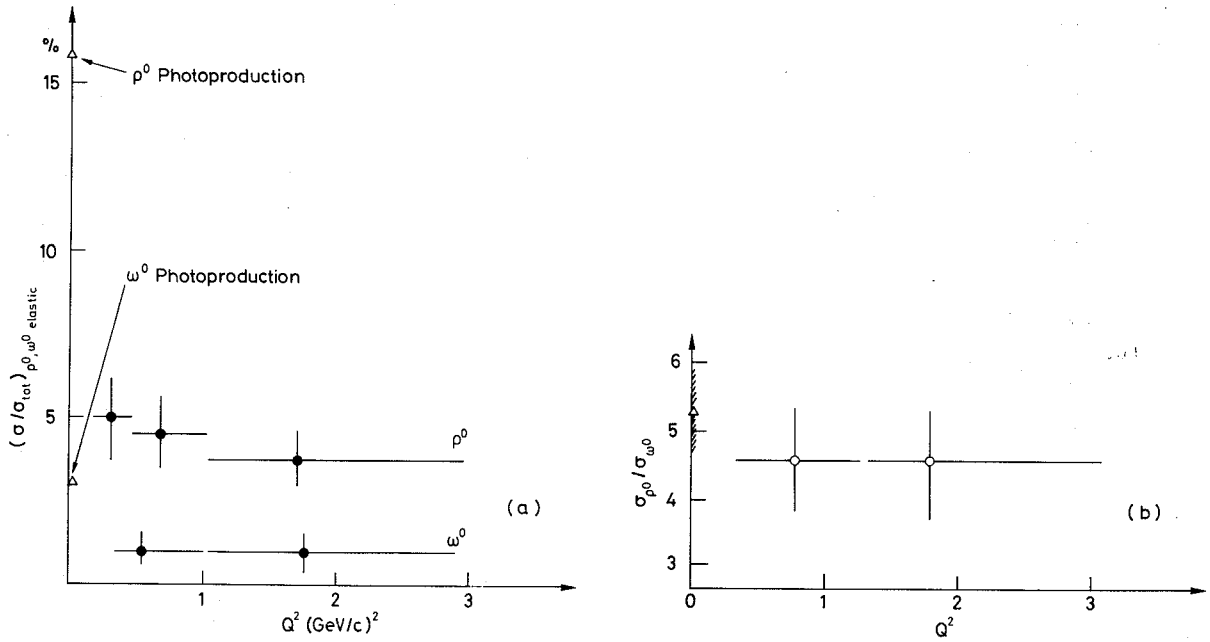

Fig. 5

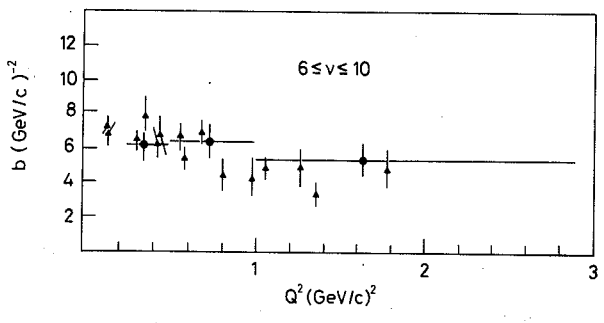

Fig. 6

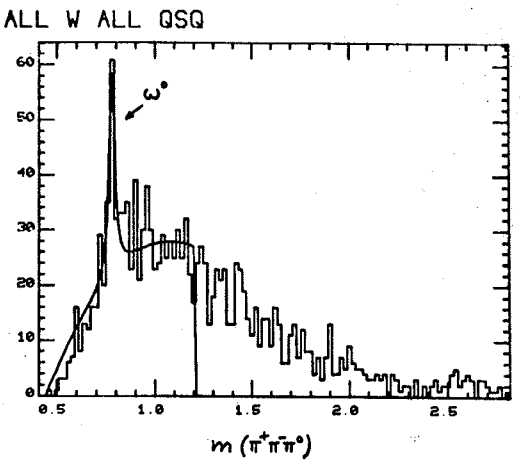

Fig. 7

sample has to be corrected for detection and reconstruction losses less well understood. Breit-Wigner fits like the one indicated in Fig. 7 lead to the $\sigma_{\omega^0}/\sigma_{tot}$ values displayed, for $W = \sqrt{s} > 2.0$, in Fig. 8 together with previously published values from a hybrid bubble chamber experiment. You will notice that our data indicate, as in the ρ^0 case, an abrupt decrease of $\sigma_\omega/\sigma_{tot}$ between $Q^2 = 0$ and $Q^2 = 0.3$, and an essentially flat Q^2 behaviour above $Q^2 = 0.3$. In Fig. 5a, we entered these data alongside the ρ^0 data and the ω^0 photoproduction value in a comparable W bin; the qualitative similarity of ρ^0 and ω^0 production is evident.

In the energy region above $W > 2$, it therefore appears that there is no basically different Q^2 trend for ρ^0 ($\mathbb{P}$ exchange) and ω^0 ($\mathbb{P}$ and π exchange) production. Remarkably, then, the SU(3)-suggested ratio for $\sigma_\rho/\sigma_\omega$ appears to remain essentially unchanged from photoproduction out to $Q^2 = 3$ electroproduction (Fig. 5b).

Let us now briefly return to the question why, in terms of individual reaction channels, σ_3/σ_{tot} dips down from its photoproduction value to a quickly reached lower plateau, which then remains constant to Q^2 of some 3 $(GeV/c)^2$: the decrease of ρ^0 and ω^0 production in the small Q^2 interval above $Q^2 = 0$ accounts for some 11% and 2%, respectively. This will account for much of the σ_3/σ_{tot} effect -- in particular, since the W bin of the reported ρ and ω data extends through the three W bins of the σ_n/σ_{tot} plot, Fig. 3. The essential flatness of σ_ρ/σ_{tot} and $\sigma_\omega/\sigma_{tot}$ over the $Q^2 > 0$ range covered in this experiment also makes the flat σ_3/σ_{tot} behaviour appear reasonable. Note, however, that the observed channel $\pi^-\Delta^{++}$ is expected to participate in the σ_ℓ turn-on (due to the π exchange amplitude), and that a balancing act will have to occur for all participating channels if $R = \sigma_t/\sigma_\ell$ for ρ^0 production is as strongly Q^2 dependent as presently believed. The final accounting, by all standards, for the participating amplitudes remains to be done.

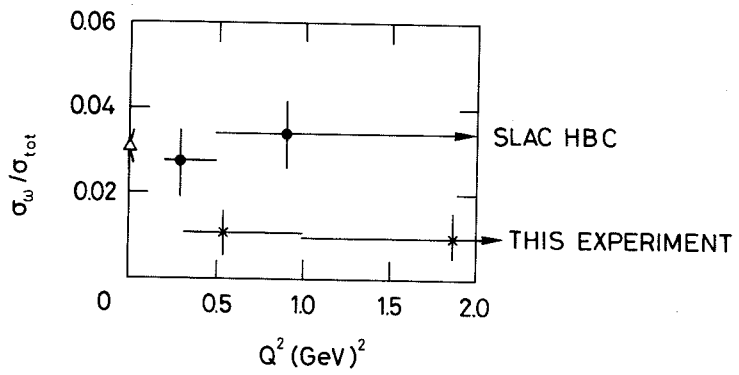

Fig. 8

4. SOME MORE GLOBAL FEATURES

I will now briefly discuss data on average multiplicities of charged hadrons, on $p_\perp$ distributions, and on the charge ratio h^+/h^- for secondary hadrons[7].

For the determination of average charged-hadron multiplicities, the condition that $n = 1, 3, 5, \ldots$, makes the correction for single lost tracks easy; the likelihood of losing two tracks was determined to be very small. The average numbers $\langle n \rangle$, displayed as a function of Q^2 in Fig. 9, show a slight but significant difference between photo- and leptoproduction in the lower $W = \sqrt{s}$ bins, with no systematic difference discernible at

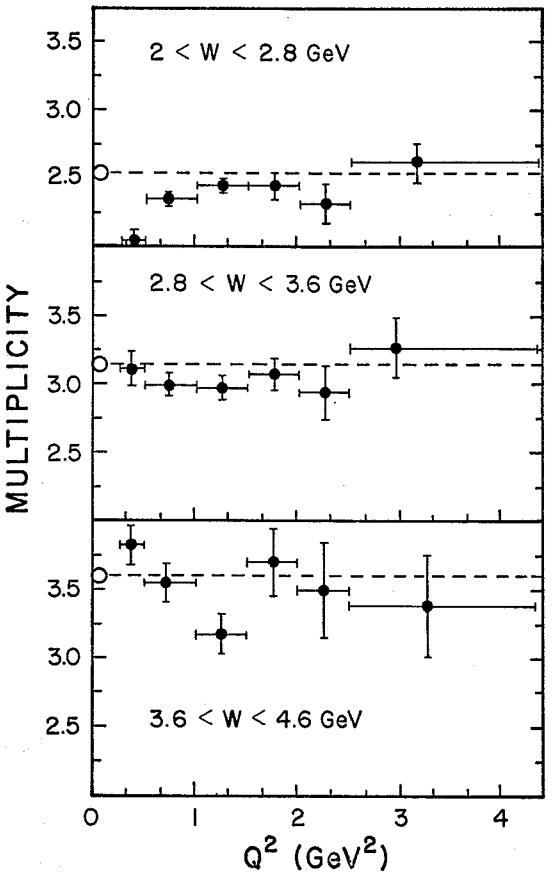

Fig. 9

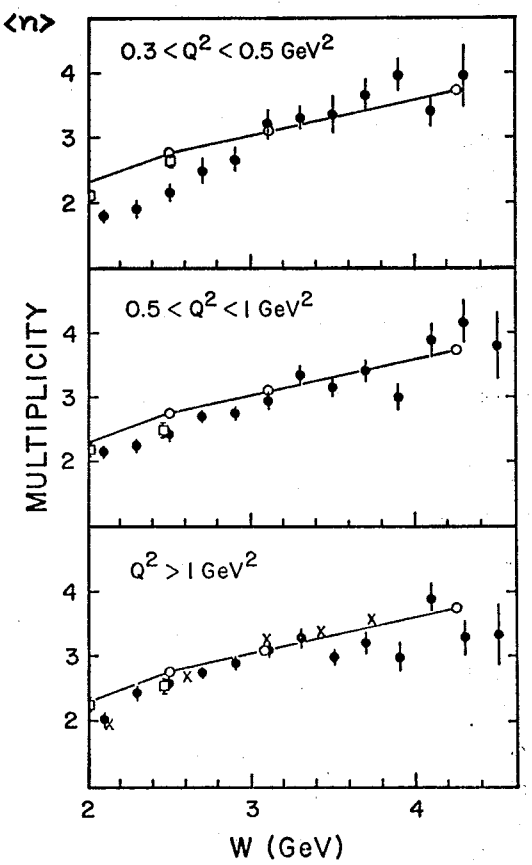

a)

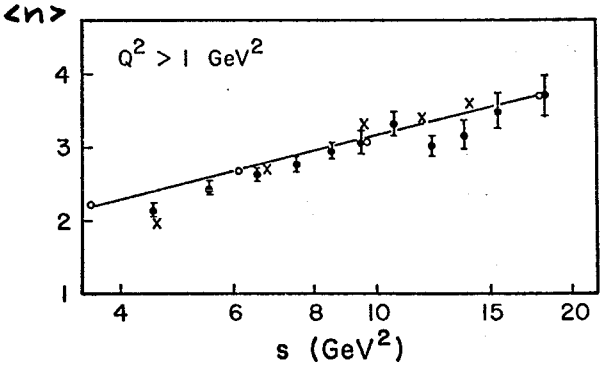

b)

Fig. 10

$s \gtrsim 20$. There is again no Q^2 trend at all for $Q^2 > 0.2$ values. The W dependence shows a clear deficit of electron versus photoproduction at values below W = 3, and possibly some structure around W = 4 (onset of ψ production?). Plotting (as in Fig. 10) the highest Q^2 bin [> 1 (GeV/c)^2] versus ln s, the dependence is seen to be reasonably close to linear. For comparison, a somewhat steeper ln s dependence resulting from a published counter experiment[10] on ep scattering is indicated by crosses. The over-all trend appears to approach that of photoproduction (solid line) with increasing energy.

These results are surprising when seen in the context of the rule suggested by Wroblewski[8], that $\langle n \rangle$ for any hadronic reaction depend only on the "Q-value" ($\approx$ the energy available for particle production)

$$\langle n \rangle = f \text{ (Q value)}$$

$$\text{Q value} \equiv \sqrt{s} - \sum m_{in} \, .$$

The "rest mass" of the virtual photon, the negative-definite quantity Q^2, changes from 0.2 to 3.0 GeV^2 in the region covered by our data, so that the Q value with $\sqrt{s}$ of, say, 3 will certainly be non-negligibly affected. The flat Q^2 behaviour of $\langle n \rangle$ therefore denies us, in this interpretation, any information on the "hadronic component" of the virtual photon that might reflect into the $\sum m_{in}$ term.

Next, we turn to transverse momentum distributions for secondaries. Figure 11a gives the $p_\perp$ distributions for positive as well as negative hadrons, for all events with $Q^2 > 0.3$ and $\sqrt{s} > 2$. These features stand out:

- for small $p_\perp^2$ ($\lesssim 0.3$), there is a steep decrease of the yield of secondaries, with exponential slopes of 8 for positives, 12 for negatives, in a fit of the form $e^{-ap_\perp^2}$;
- for larger $p_\perp^2$ values (up to ~ 0.8), an exponential fit of one-half these slopes appears to describe the data well;
- the average transverse momentum imparted to a secondary hadron is different for positives and negatives, but not dependent on $Q^2 > 0.2$ (Fig. 11b).

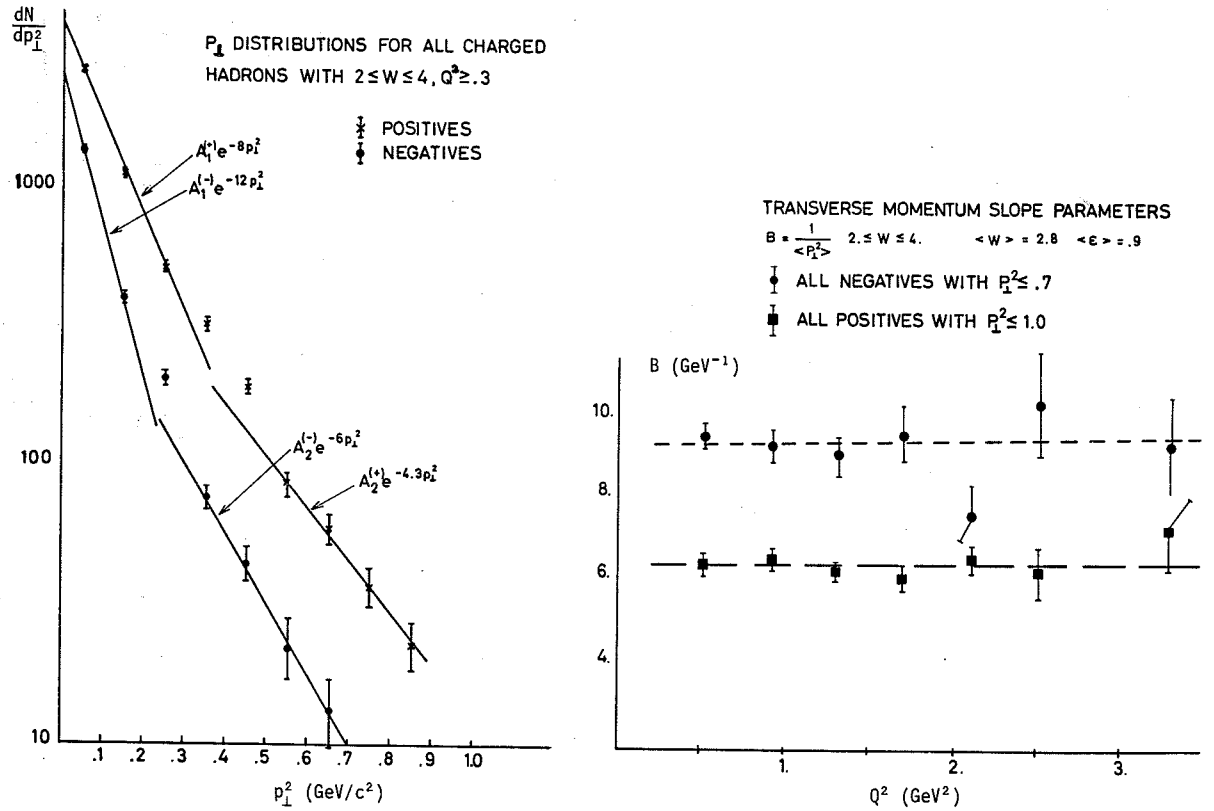

Fig. 11

Turning now to the charge ratios for secondary hadrons, you may remember that at the time of the 1974 London Conference, there appeared to be a strong trend for the π^+/π^- ratio for forward-emitted hadrons to keep increasing with Q^2, reinforced by preliminary data from this experiment. The implications of this phenomenon on the quark-parton picture had been stressed by Dakin and Feldman[9].

Forward means a cut-off in the fractional longitudinal momentum x. In this experiment, however, there is no reliable way to separate π from K and p; therefore, the wrong assumption of a particle's rest mass may well lead to its completely erroneous assignment of an x value, and therefore faulty binning. For strongly forward particles, the nucleon admixture is negligibly small, so that the hadronic charge ratio

$$h^+/h^- \approx \pi^+/\pi^- \quad \text{for} \quad x \gtrsim 0.3 \ .$$

For data including smaller x values, we have to remind ourselves that

$$h^+ = \pi^+ + K^+ + p$$
$$h^- = \pi^- + K^-$$

where we have to beware of binning in the variable x. For some comparisons, it may be useful to remove one-prong events since they contain the purely protonic final state $p\pi^0$.

With these caveats, look at Fig. 12: we purposely chose only higher-energy events (W > 3) to illustrate the trend (smaller W bins may be more strongly affected by faulty particle mass assignment). While there is still clear evidence for Q^2 dependence of $R = \pi^+/\pi^-$ (for x > 0.3), it may well be that a saturation value of about 2 has been reached at $Q^2 \sim 1$. To check on this point, we removed all one-prong events from the sample, and found a behaviour consistent with Q^2 independence starting at even lower Q^2 values (Fig. 12b). Remember, however, that the specification of the kinematic bin is important when comparisons with other data are made (lower-s data have a higher R).

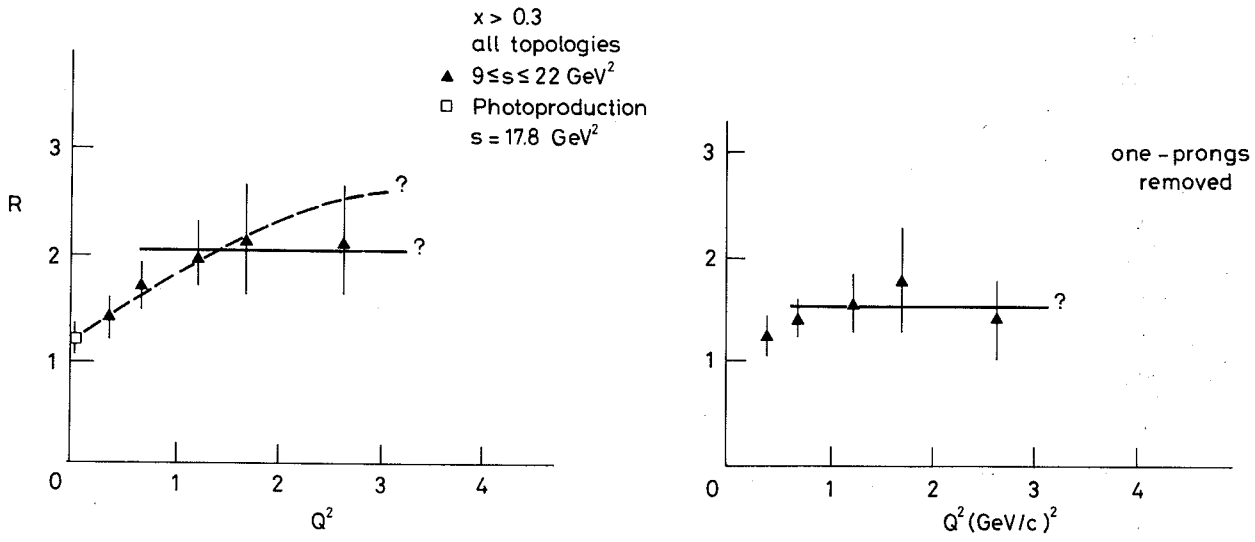

Fig. 12

The energy dependence of R is shown in Fig. 13, again for x > 0.3. The lower-s sample is probably somewhat distorted from misidentification; however, the trend is clear:

- strong s dependence at lower energies
- approach to the R value of the full (all-x) sample given by the mean multiplicity according to

$$R_{(\text{all } x)} = \frac{\langle n \rangle + 1}{\langle n \rangle - 1}$$

with one-prongs removed, R (x > 0.3) will then clearly fall below this $R_{(all\ x)}$ value (Fig. 13b).

Finally, we show the dependence of R on transverse momentum. In Figs. 14a to 14d, a remarkable feature stands out: whereas the $p_\perp$ trend appears to be a weak one for the forward (x > 0.3) sample, the full sample, dominated by small-x particles, shows a definite trend for an increase of $R_{(all\ x)}$ with $p_\perp$. Looking at Figs. 14a and 14c, we may even speculate that, at higher s values, the $p_\perp$ dependence becomes s independent.

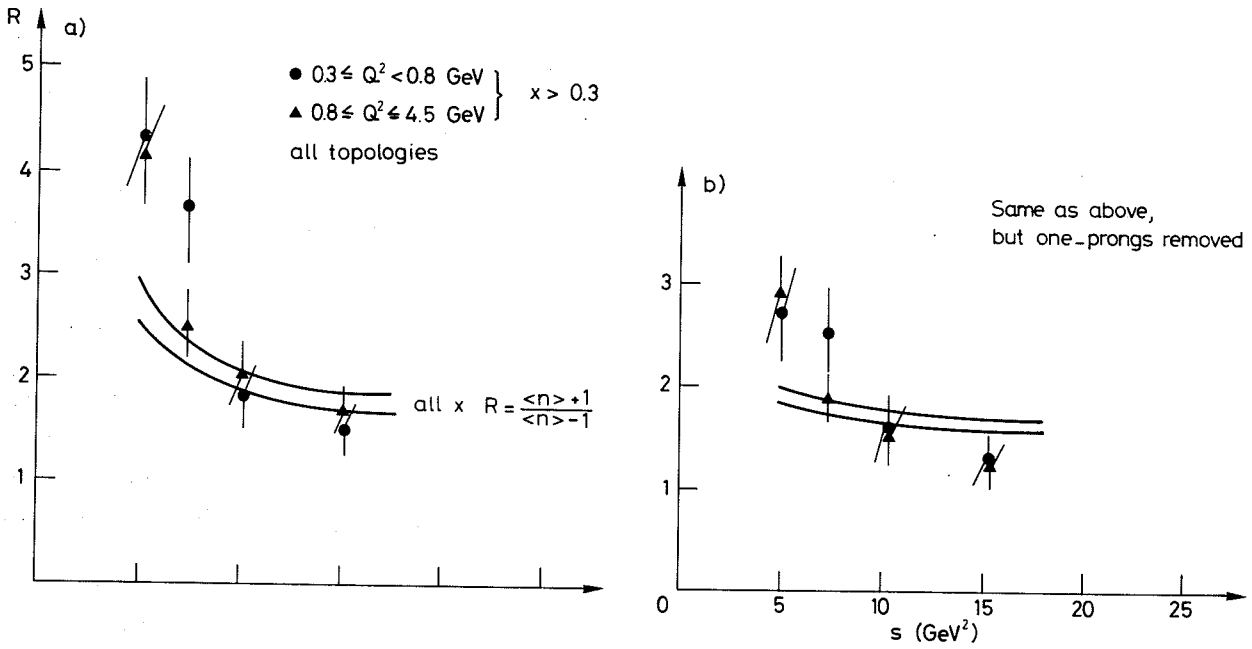

Fig. 13

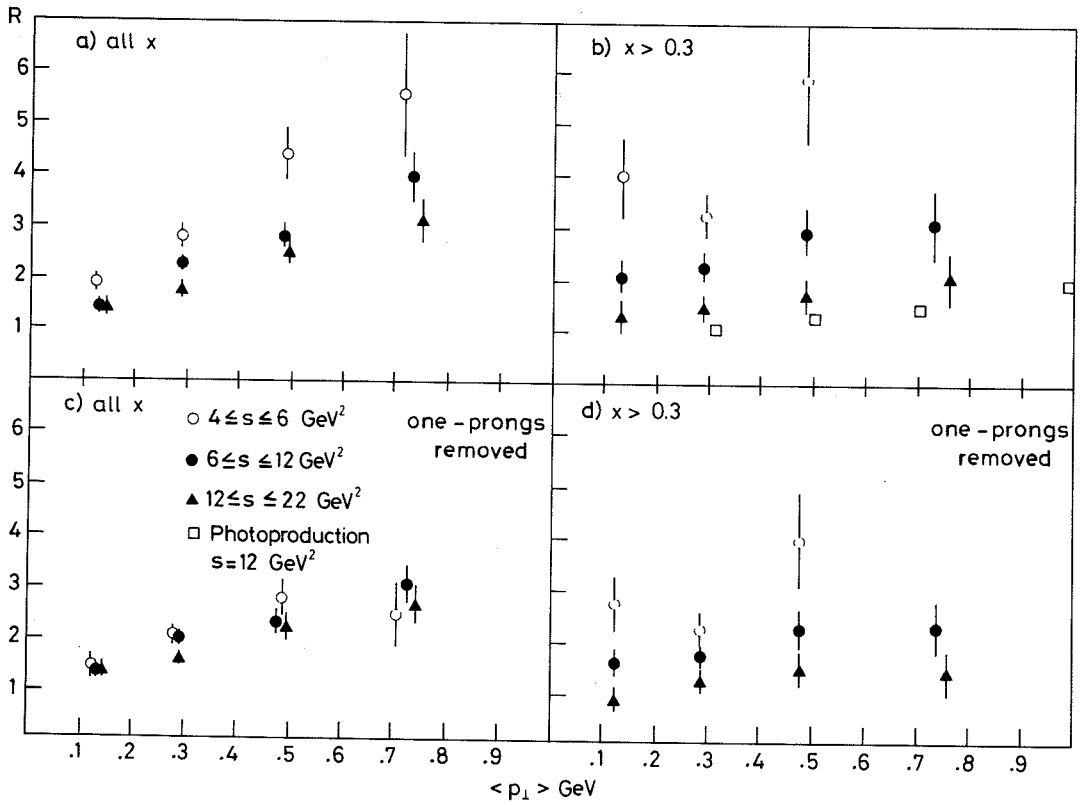

Fig. 14

This feature may be looked at in two ways: First, consider a large-$p_\perp$ event:

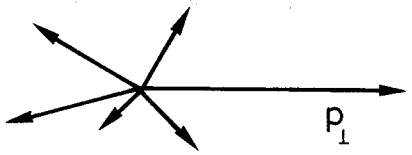

The mass of the "recoiling " system is relatively small, the multiplicity correspondingly low. R is therefore large, as shown in Fig. 13. It is not presently clear whether this mechanism can explain the observed increase of R with $p_\perp$ quantitatively.

We therefore turn to a second, much more exciting possibility: in the central rapidity region whose population dominates these plots, the identity of the partons hit by the virtual photon has no influence. It is therefore possible to speculate that we see here another manifestation of the virtual photon treating different charges differently -- not behaving in an isospin-invariant way when "creating" hadrons. Remember that, after all, the observation of different νW^2 values for ep and en scattering have long given similar indications.

5. CONCLUSIONS

Are these data bringing us any closer to understanding how the scaling behaviour of the inelastic structure functions νW_2, W_1 is built up from individual constituent processes?

The pattern emerging is fairly consistent, but it does not give us a clue as to why ω should be the scaling variable: $\langle n \rangle$, $\langle p_\perp \rangle$, σ_n/σ_{tot} all appear to be fairly independent of Q^2 in the scaling region; ρ^0 and ω^0 "elastic" production appear to constitute a fairly Q^2-independent fraction of the total inelastic cross-section up to Q^2 values of 3 (we have no information beyond), down by about a factor of 3 from photoproduction. Even the forward charge ratio π^+/π^- may tend to plateau at moderate Q^2 values. None of these quantities appear to seek out ω as the significant variable.

It may be that we need a wider Q^2 range to convince us of the correctness of the picture as it presents itself today. In the meantime, any description of the virtual photon-hadron coupling will have to keep in mind these newly emerging features:

- γ_V appears to retain some memory of the SU(3) structure of the real photon, up to higher Q^2 values;
- γ_V treats hadrons in a charge-asymmetric way: not only is $\nu W_2^{(n)} \neq \nu W_2^{(p)}$, but also $R \equiv h^+/h^-$ increases noticeably with $p_\perp$ in the central rapidity region.

REFERENCES

1) Its members are: K. Bunnell, C. del Papa, D. Dorfan, M. Duong-van, S. Flatté, B. Lieberman, G. Luxton, H. Meyer, L. Moss, R. Mozley, A. Odian, T. Schalk, A. Seiden, F. Villa and L.C. Wang.

2) S. Flatté, C.A. Heusch and A. Seiden, Nuclear Instrum. Methods 119, 333 (1974).

3) C.A. Heusch, B. Lieberman and A. Seiden, Nuclear Instrum. Methods 124, 165 (1975).

4) U. Koetz, communication to this Conference.

5) R. Talman, Proc. 6th Int. Symposium on Electron and Photon Interactions at High Energies, Bonn (1973).

6) L. Osborne, private communication. Relevant data from the present experiment are in preparation.

7) Preliminary results had been presented to the 17th Int. Conf. on High-Energy Physics, 1974 (Proc. pp. IV 65, IV 72).

8) A. Wroblewski, 4th Int. Symposium on Multiparticle Hadrodynamics, Pavia (1973).

9) J. Dakin and G. Feldman, Phys. Rev. Letters D8, 2862 (1973).

10) P.H. Garbincius, K. Berkelman, B. Gibbard, J.S. Klinger, P. Wanderer and A.J. Sadoff, Phys. Rev. Letters 32, 328 (1974).